TOWARDS POINT-OF-CARE MEDICAL APPLICATIONS USING ELECTROCHEMICAL BIOSENSORS

Elena Alina CHITICARU[1], Georgian Alin TOADER[1,*], Mariana IONIȚĂ[1,2,3]

Glassy carbon electrodes (GCEs) and screen-printed carbon electrodes (SPCEs) were successfully modified with graphene oxide (GO) for rapid DNA detection. Transmission electron microscopy (TEM), Raman spectroscopy, Fourier transform infrared spectroscopy, and X-ray diffraction were used to characterize the GO dispersion used for the aforementioned purpose. Furthermore, the results from electrochemical impedance spectroscopy (EIS) and cyclic voltammetry (CV) indicated that while both GO-GCEs and GO-SPCEs platforms demonstrated good DNA adsorption capabilities, GO-SPCEs exhibited a higher sensitivity for DNA hybridization detection. This property of GO-SPCEs is of paramount importance in point-of-care applications, enabling the potential to make healthcare more accessible, efficient, and patient-centred.

Keywords: electrochemistry, graphene oxide, DNA detection, glassy carbon electrode, screen-printed carbon electrode

1. Introduction

The increasing number of genetic analyses is driving rapid advancement in biosensor technologies that enable fast and economical identification of particular deoxyribonucleic acid (DNA) sequences related to a wide range of human diseases. Various approaches, such as optical techniques [1-3], piezoelectric [4, 5], and electrochemical methods [6, 7], have been proposed for DNA detection systems. The electrochemical method stands out among these techniques for its widespread implementation, primarily because of its remarkable simplicity, sensitivity, rapidity, and affordability [8, 9]. Furthermore, it presents the added advantage of enabling the development of self-powered miniaturized devices, which hold great relevance for real-time diagnostics applications [10-12].

Concentrated efforts have been put into developing biosensors for nucleic acids built on several electrochemical approaches, like cyclic voltammetry (CV), differential pulse voltammetry (DPV), square-wave voltammetry (SWV), electrochemiluminescence (ECL), electrochemical impedance spectroscopy (EIS),

[1] Faculty of Medical Engineering, The National University of Science and Technology POLITEHNICA Bucharest, Romania, *corresponding author: georgian.toader3007@upb.ro
[2] Advanced Polymer Materials Group, The National University of Science and Technology POLITEHNICA Bucharest, Romania
[3] eBio-Hub Research Centre, The National University of Science and Technology POLITEHNICA Bucharest, Romania

etc. As an electrochemical detection method, EIS is often the preferred choice because it can effectively identify significant signal changes within a low concentration range for the target analyte. Moreover, EIS is a non-destructive tool as it employs smaller-amplitude voltage perturbations, which are substantially lower than those used in amperometric analysis [13, 14].

Several nanomaterials have been used so far in electrochemical sensing [15]. Among these, graphene has been extensively investigated for this purpose because of its remarkable properties, such as increased surface to volume ratio, thermal and chemical stability, high carrier mobility and electrical conductivity [6]. DNA molecules can be attached onto the graphene layer through covalent or non-covalent interactions. The immobilization of DNA through physical adsorption on GO surface predominantly relies on noncovalent interactions, specifically pi stacking between DNA aromatic rings and the carbonic hexagonal rings present in the graphenic structure [10].

Carbonic materials have been employed as working-electrodes (WE) in electrochemistry for decades, benefiting from various advantages such as versatility in selecting redox active probes, non-toxicity, a stability, wide potential window, chemical inertness, and cost-effectiveness [16]. Glassy carbon electrodes (GCE) are traditional electrode materials that consist of a polished glassy carbon surface. These electrodes can be modified to increase their surface area, facilitating an efficient immobilization of ssDNA probes and promoting a selective and sensitive detection [17]. Nonetheless, the fabrication process of biosensors based on GCE can be laborious, time-consuming and may necessitate extra preparation steps before use.

Conversely, SPCEs have earned increasing attention due to their affordability, portability, and ease of operation, making them convenient for mass production of reproducible and high-quality biosensors, particularly for point-of-care biomedical applications [18-20]. Although both SPCEs and graphene have been intensively investigated, there is poor research available on the mass manufacture of these electrochemical biosensing platforms.

This study presents the fabrication of a detection electrochemical platform derived from GCE modified with GO (GO/GCE) for comparison with GO modified SPCE (GO/SPCE) for the rapid identification of DNA hybridization. Both classes of electrodes were modified with GO in the same conditions and further optimization of the protocol was conducted on the classical well-known GCEs. The experimental conditions obtained on GCEs were then applied on SPCEs to determine if a similar or better response could be obtained and therefore to pave the way for miniaturized, portable biosensing devices. GO dispersion prepared by ultrasonication was extensively characterized by several techniques, such as Transmission Electron Microscopy (TEM), Raman and Fourier Transform Infrared (FTIR) spectroscopy, X-ray diffraction (XRD), and all confirming the quality of the

nanomaterial used to modify the electrodes. The bioreceptor (ssDNA probe) was immobilized on both electrodes by physisorption and the hybridization with the target molecule was investigated by both EIS and CV in the presence of a redox system. Our results show that DNA probe was successfully immobilized on both electrodes, while the hybridization event was detected with a higher sensitivity on SPCE.

2. Materials and methods

The reagents utilized in this research included GO in H_2O (2 mg/mL), HNa_2O_4P, H_2NaO_4P, KCl, $K_4[Fe(CN)_6] \times 3H_2O$, $K_3[Fe(CN)_6]$, and HCl, had been bought through Merck Co. (Darmstadt, Germany) and Sigma-Aldrich (St. Louis, MO, USA). The IDTE buffer, ssDNA probe (5'-TTTCAACATCAGTCTGAT AAGCTATCTCCC-3'), together with its ssDNA target (5'-GGGAGATAGCTT ATCAGACTGATGTTGAAA-3') had been procured through Integrated DNA Technologies, Inc. (Coralville, IA, USA). The electrodes used in the experiment were washed before and after any modifications using ultrapure water from an water purification system Crystal EX Adrona (resistivity of 18.2 MΩ × cm).

Electrochemical analysis was performed utilizing a system composed of three-electrode containing a saturated Ag/AgCl reference electrode, a platinum wire as auxiliary electrode and a WE as GCE (3 mm diameter). GCE was cleaned with 0.3 μm fine particles alumina on micro-cloth pads before use. Screen-printed carbon electrodes (SPCE-DRP 110) had been acquired through Metrohm DropSens, Spain and have integrated a silver pseudo-reference electrode, a 4 mm diameter WE, and counter electrode (carbon). To minimize electromagnetic interference, the measurements were performed inside a Faraday cage (Metrohm Autolab, the Netherlands). All electrochemical measurements were recorded in 0.1M KCl electrolyte solution containing 1 mM $[Fe(CN)_6]^{3-/4-}$, unless stated otherwise. EIS was performed at a frequency between 0.01 and 10^5 Hz, an amplitude of 10 mV AC, applying the formal potential between the redox system and the pseudo-reference. If the electrodes were not used immediately, they were stored at 4°C.

Both GCE and SPCE were modified with 0.3 mg/mL GO by drop-casting 2 μL and 3 μL GO dispersion, respectively, and each of them was dried for 2 hours at 60°C. Prior to GO modification, SPCE was pretreated to enhance its electrochemical properties. The electrodes underwent five CV cycles at a sweep rate of 0.05 V/s, at a potential range between +0.5 V and -1.5 V in 0.1 M HCl and five more CV cycles between 0 V and +2 V in a phosphate buffer solution (0.1 M PBS, pH 7).

The bioreceptor consisting of ssDNA probe was immobilized on GO/GCE and GO/SPCEs by physical adsorption, incubating the electrodes with 10 μL

ssDNA solution for 4 hours at room temperature. The hybridization with DNA target was conducted by immersing the functionalized electrodes with 10 µL target-DNA mixture for minimum 2 hours at room temperature.

GO dispersion was prepared by utrasonication for 1 hour and then characterized by TEM, XRD, FTIR, and Raman spectroscopy. TEM images were obtained with a high-resolution transmission electron microscope Tecnai G2 F30 S-TWIN (ThermoFisher, Eindhoven-Nederlands) operated at 300 kV. XRD investigation on GO was performed with a Rigaku SmartLab equipment (Rigaku Corp., Tokyo, Japan), used at 200 mA and 45 kV, parallel-beam configuration (2θ/θ scan-mode), and CuKα radiation (1.54059 Å). FTIR measurements on GO sample were performed with a Vertex 70 Bruker FTIR spectrometer incorporating attenuated-total-reflectance (ATR) component. Thirty-two scans were registered at room temperature in the ATR-FTIR mode with a 4 cm^{-1} resolution in the 600 – 4000 cm^{-1} wavenumber range. Raman investigation was conducted using a confocal inVia-Renishaw Raman spectrometer (Renishaw, Brno-Cernovic, Czech-Republic), 5% laser power, 633 nm laser excitation, and the 100× objective.

3. Results and discussions

3.1. Graphene oxide characterization

Structural investigations on GO were conducted by FTIR, Raman spectroscopy, and XRD. The FTIR spectrum of the GO dispersion used to modify the electrodes is shown in Fig. 1 (A). The main peaks of the GO spectrum at 1133 cm^{-1}, 1750 cm^{-1}, and 3438 cm^{-1} correspond to the carboxyl (COOH) groups that include the C-OH vibrations. Additionally, the peaks at 1384 cm^{-1} and within the range of 1600-1650 cm^{-1} indicate the vibration modes of epoxide (C-O-C) along with the sp^2 carbon of the ketonic species (C=C). The weak vibration modes at 2853 cm^{-1} and 2927 cm^{-1} stand for the symmetric and asymmetric vibrations, respectively, of the C-H stretching groups. These are typical bands recorded for GO as reported in the scientific literature [21, 22]. Raman spectroscopy is another technique that offers valuable insights into the structural features of GO. The distinctive bands of GO are represented in Fig. 1 (B) by the D band at 1333 cm^{-1} and the G band at 1605 cm^{-1}, in accordance with [23, 24]. These bands correspond to the structural disorder and the bond-stretching of sp^2 carbon atoms, respectively. The ID/IG ratio, obtained by analyzing the intensities of D and G bands is measured at 1.14. Additionally, other bands, such as 2D and D + D′, emerge due to defects within the graphenic structure. Moreover, the XRD profile of the GO probe is presented in Fig. 1 (C). A distinct and broad diffraction peak at 2θ=10.73° specific to GO was observed in the XRD pattern, corresponding to the (001) reflection plane [25-27]. The GO sample morphology was examined by TEM (Fig. 1 D), revealing a transparent laminated GO sheet with only a few layers and the typical wrinkled

and folded pattern usually observed for this material [28, 29]. The GO dispersion with aforementioned features was further used for electrodes modification according to the procedure described in section 2.

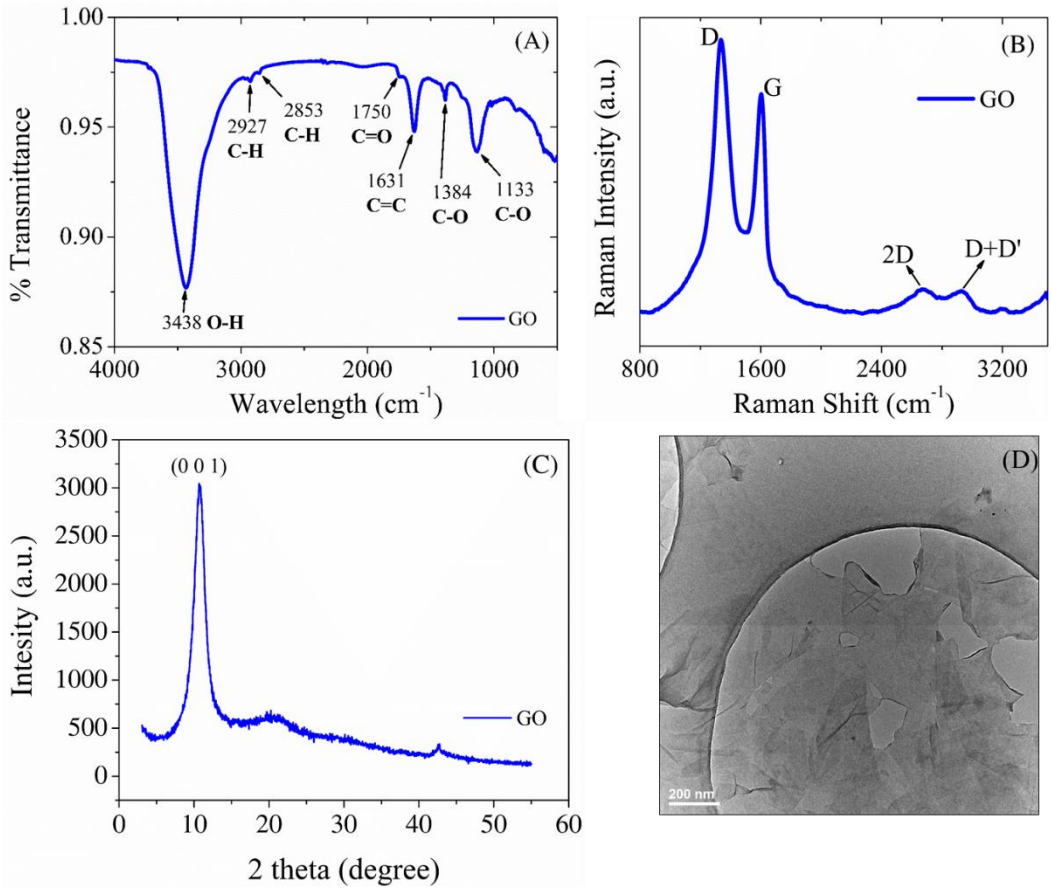

Fig. 1. (A) FTIR, (B) Raman spectroscopy, (C) XRD, and (D) TEM analysis of GO dispersion.

3.2. Electrochemical measurements and characterization

3.2.1. Electrochemical characterization of GO-modified electrodes

3.2.1.1. GCE modification with GO dispersion

A GCE was firstly cleaned and then modified with GO dispersion as depicted in section 2. Fig. 2 shows the electrochemical properties of GCE before and after GO modification. CV recordings (Fig. 2 A) in presence of 1mM $[Fe(CN)_6]^{3-/4-}$ redox probe show a curve with well-defined oxido-reduction peaks for the bare GCE, having a current intensity of 21.34 µA and a peak to peak separation potential (ΔEp) of 130 mV. GCE modification with GO by drop-casting

induced a decrease in peak current intensity with 5.16 µA while ΔEp did not change. EIS measurements (Fig. 2 B) are in accordance with CV, showing a low Rct for the unmodified GCE of approximatively 1.9 kΩ, which increases to 4.9 kΩ after deposition of GO on the electrode surface. The electrochemical response confirms the modification of GCE with GO dispersion.

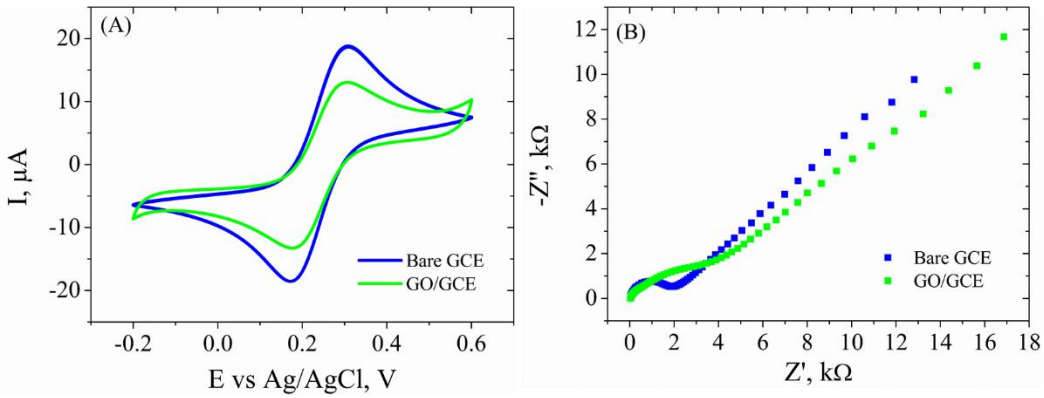

Fig. 2. (A) CV and (B) EIS Nyquist plot, recorded in 0.1M KCl containing 1 mM $[Fe(CN)_6]^{3-/4-}$, for bare GCE and GO/GCE. EIS was performed in the frequency range of 0.01-10^5 Hz.

3.2.1.2. SPCE modification with GO dispersion

The electrochemical properties were also recorded for SPCE before and after each modification (Fig. 3). On the one hand, it is observed in CV (Fig. 3 A) that the commercial SPCE as received has a relatively low current intensity (22.7 µA) and a large ΔEp of 240 mV. These properties were substantially improved after the electrochemical treatment in HCl and PBS, measuring an increase in the anodic peak intensity up to 32 µA and a significant decrease in ΔEp (110 mV). The deposition of GO dispersion on the SPCE surface caused a decrease in current intensity with 16 µA and an enlargement with 40 mV of the peak-to-peak separation potential. On the other hand, impedimetric measurements (Fig. 3 B) reveal a charge transfer resistance of 3.9 kΩ for the unmodified electrode with a well-defined semicircle, that is visibly reduced (to 1.6 kΩ) after the pretreatment. Finally, GO modification increased Rct to 6.2 kΩ, expected behavior due to the low-conductive behavior of the nanomaterial and confirms the results obtained on GCEs.

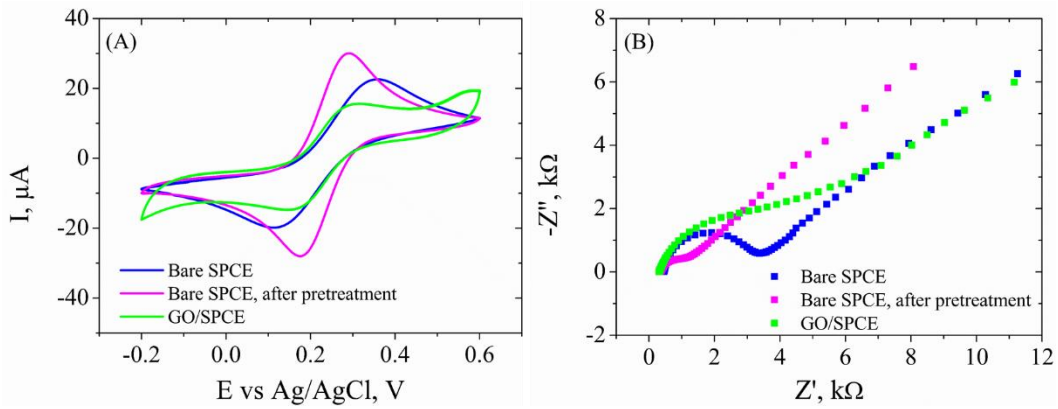

Fig. 3. (A) CV and (B) EIS Nyquist plot, recorded in 0.1M KCl containing 1 mM $[Fe(CN)_6]^{3-/4-}$, for bare SPCE, SPCE after electrochemical pretreatment, and GO/SPCE. EIS was performed in the frequency range of 0.01-10^5 Hz.

3.2.2. Characterization, testing and comparison of the sensing platforms

3.2.2.1. DNAp-GO/GCE response towards DNA hybridization

Several concentrations of ssDNA probe were immobilized on GO-modified GCEs in order to determine the saturation level and ensure that the electrode surface is completely covered with oligonucleotides. To this end, GO/GCE was incubated with 25 nM, 50 nM, 100 nM, 500 nM, and 10 µM DNA probe, respectively, at room temperature for 4 hours each. CV recordings (Fig. 4 A) show successive decreases in current intensity with each DNA probe incubation, from 16 µA corresponding to GO/GCE, to 10 µA for 500 nM DNA probe and 9.45 µA for 10 µM DNA probe. At the same time, the peak-to-peak separation potential increased from 140 mV (measured for GO/GCE) to 210 mV, 214 mV, 240 mV, and 260 mV, respectively, with each DNA probe concentration immobilized on the electrode surface. EIS measurements presented in the form of Nyquist plot (Fig. 4 B) are in accordance with CV results, showing an increase in Rct with each immobilization of DNA probe. The charge transfer resistance increased from 4.9 kΩ (GO/GCE) to 8.7 kΩ, 9.8 kΩ, 10.5 kΩ, 13.4 kΩ, and 13.3 kΩ after successive incubations in 25 nM, 50 nM, 100 nM, 500 nM, and 10 µM DNA probe, respectively. Both electrochemical measurements confirm the successful immobilization of the bioreceptor on the electrode surface and show that a level of saturation was achieved. The decrease in current intensity along with the increase in charge transfer resistance upon DNA probe immobilization explained by the repellence between $[Fe(CN)_6]^{3-/4-}$ and the negatively charged DNA molecules.

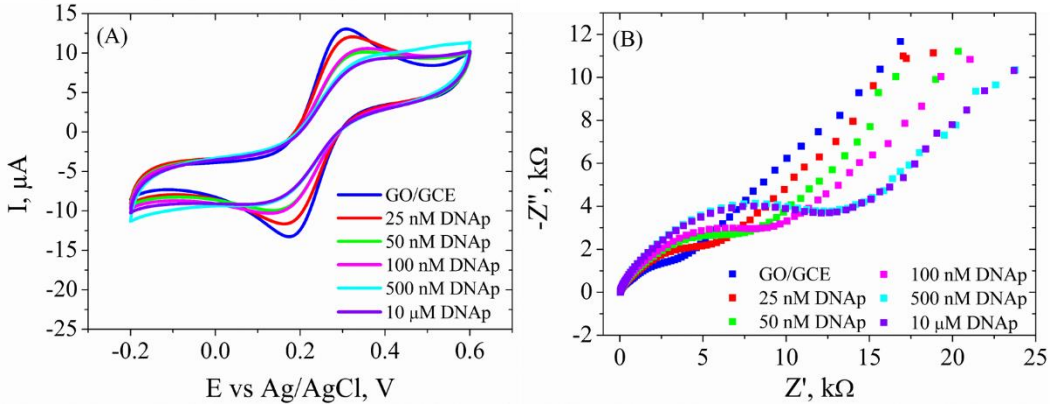

Fig. 4. (A) CV and (B) EIS Nyquist plot, recorded in 0.1M KCl containing 1 mM $[Fe(CN)_6]^{3-/4-}$, for GO/GCE and for GO/GCE after incubation with 25 nM, 50 nM, 100 nM, 500 nM, and 10 µM DNA probe. EIS was performed in the frequency range of 0.01-10^5 Hz.

The hybridization event was conducted between the functionalized DNAp-GO/GCE and single-stranded DNA target by incubating the electrode with several concentrations of DNA target (10 nM – 500 nM) for minimum 2 hours at room temperature, monitoring the changes in the electrochemical signal in the presence of ferri/ferrocyanide as a redox indicator. The following characterization of the electrodes by CV (Fig. 5 A) reveals an increase in the peak currents with each DNA target incubation, from 9.45 µA (DNAp-GO/GCE) to 11.7 µA after incubation in 10 nM DNA target, 12.28 µA after hybridization with 50 nM DNA target, 12.9 µA following incubation in 100 nM DNA target, and 13 µA when the functionalized electrode was hybridized with 500 nM DNA target. Impedimetric measurements (Fig. 5 B) in this case show small changes in Rct following each incubation with DNA target, decreasing from 13.3 kΩ (DNAp-GO/GCE) to 13 kΩ, 12.9 kΩ, 12.7 kΩ and 12.5 kΩ after incubation with 10 nM, 50 nM, 100 nM, and 500 nM DNA target, respectively. This trend observed in the electrochemical signal is a consequence of the weak interactions between GO and double-stranded DNA, that facilitates the rapid desorption of the hybridized DNA probe.

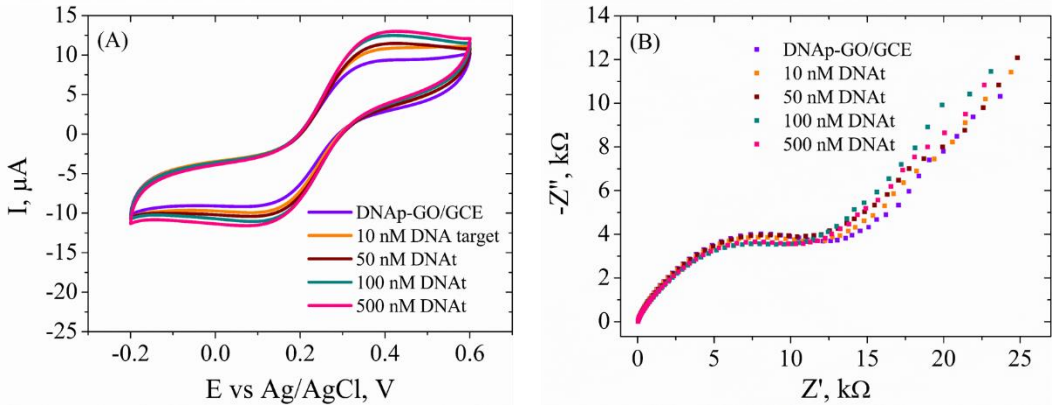

Fig. 5. (A) CV and (B) EIS Nyquist plot, recorded in 0.1M KCl containing 1 mM $[Fe(CN)_6]^{3-/4-}$, for DNAp-GO/GCE and after incubation with 10 nM, 50 nM, 100 nM, and 500 nM DNA target. EIS was performed in the frequency range of 0.01-10^5 Hz.

3.2.2.2. DNAp-GO/SPCE response towards DNA hybridization

Following the studies performed on GCEs, the same procedure was followed for SPCEs modified with GO dispersion using 10 µM DNA probe and 500 nM DNA target to determine if the response in the electrochemical signal is similar. CV analysis (Fig. 6 A) reveals an increase of the current intensity from 15.69 µA of the GO/SPCE to 16.27 µA after the modified electrode was incubated with DNA probe for 4 hours at room temperature. Moreover, following the hybridization of DNAp-GO/SPCE with 500 nM DNA target, the intensity of the current peaks dropped to 15.75 µA. It is observed that on this type of electrodes the response in CV is not as sensitive as the one obtained on GCE, however the trend in the electrochemical signal is the same. The impedimetric measurements (Fig. 6 B) reveal a more sensitive response after incubation of DNAp-GO/SPCE with 10 µM DNA probe, the charge transfer resistance increasing from 6.2 kΩ (corresponding to GO/SPCE) to 10.7 Ω, indicating the effective immobilization of the bioreceptor on the modified electrode. Next, the hybridization with 500 nM DNA target induced a decrease in Rct down to 7.2 kΩ, clearly showing the weaker affinity of double-stranded DNA for GO, which determined the desorption of the biomolecule from the electrode surface.

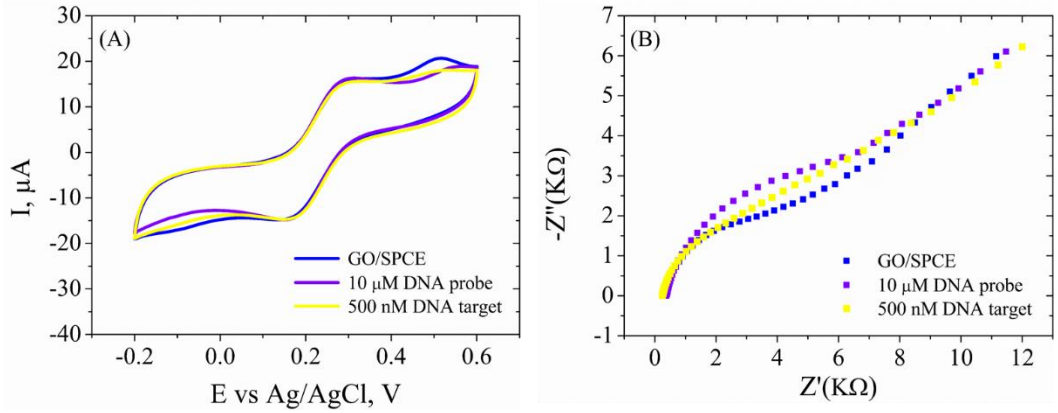

Fig. 6. (A) CV and (B) EIS Nyquist plot, recorded in 0.1M KCl containing 1 mM $[Fe(CN)_6]^{3-/4-}$, for GO/SPCE, GO/SPCE incubated with 10 µM DNA probe and after hybridization with 500 nM DNA target. EIS was performed in the frequency range of 0.01-10^5 Hz.

4. Conclusions

This study shows the successful development of electrochemical detection platforms for the rapid detection of DNA hybridization, using graphene oxide modified GCEs and SPCEs. The experimental conditions optimized on classical GCEs were applied to SPCEs, aiming to enable the development of miniaturized and portable biosensing devices.

Before electrode modification, graphene oxide underwent a thorough characterization using FTIR, Raman spectroscopy, XRD, and TEM, all these techniques showcasing its excellent dispersion, consisting of one to a few layers, and revealing the existence of typical functional groups on the lattice. Both GO/GCE and GO/SPCE platforms demonstrated successful immobilization of the bioreceptor, a ssDNA probe, through physical adsorption. Furthermore, the hybridization event within the ssDNA probe and its complementary target DNA was efficiently detected by electrochemical tools such as CV and EIS, in the presence of a ferri/ferrocyanide redox system. Notably, the GO/SPCE platform exhibited higher sensitivity in EIS for detecting DNA hybridization, while GO/GCE showed a more sensitive response in CV after the DNA hybridization event.

This research contributes valuable insights into the development and application of electrochemical biosensors based on graphene, particularly in the context of DNA detection. The findings open doors to the realization of compact and portable biosensing devices, which could have significant implications in various fields, such as medical diagnostics, environmental monitoring, and POC testing. Further advancements in nanomaterial-based biosensors hold promise for

addressing real-world challenges and improving the selectivity and sensitivity for nucleic acid detection technologies.

Funding

This work was supported by a grant of the Ministry of Research, Innovation and Digitization, Executive Agency for Higher Education, Research, Development and Innovation, project number PCE 103/2022 (REOSTEOKIT) and by Ministry of Research and Innovation, Operational Program Competitiveness Axis 1 - Section E, Program co-financed from European Regional Development Fund "Investments for your future" under the project number 154/25.11.2016, P_37_221/2015, “A novel graphene biosensor testing osteogenic potency; capturing best stem cell performance for regenerative medicine” (GRABTOP).

R E F E R E N C E S

[1] F. R. Nitu, J. S. Burns, and M. Ionită, "Oligonucleotide Detection and Optical Measurement with Graphene Oxide in the Presence of Bovine Serum Albumin Enabled by Use of Surfactants and Salts," Coatings, vol. 10, p. 420, 2020.

[2] F. R. Nitu, L. Savu, S. Muraru, I. Stoian, and M. Ionita, "Label-Free Homogeneous microRNA Detection in Cell Culture Medium Based on Graphene Oxide and Specific Fluorescence Quenching," Nanomaterials (Basel), vol. 11, Feb 2 2021.

[3] F. Khozeymeh, F. Melli, S. Capodaglio, R. Corradini, F. Benabid, L. Vincetti, et al., "Hollow-Core Fiber-Based Biosensor: A Platform for Lab-in-Fiber Optical Biosensors for DNA Detection," Sensors (Basel), vol. 22, Jul 8 2022.

[4] M. Pohanka, "Overview of Piezoelectric Biosensors, Immunosensors and DNA Sensors and Their Applications," Materials (Basel), vol. 11, Mar 19 2018.

[5] T. Wasilewski, D. Neubauer, M. Wojciechowski, B. Szulczyński, J. Gębicki, and W. Kamysz, "Evaluation of Linkers’ Influence on Peptide-Based Piezoelectric Biosensors’ Sensitivity to Aldehydes in the Gas Phase," International Journal of Molecular Sciences, vol. 24, p. 10610, 2023.

[6] G. Ashraf, A. Aziz, T. Iftikhar, Z.-T. Zhong, M. Asif, and W. Chen, "The Roadmap of Graphene-Based Sensors: Electrochemical Methods for Bioanalytical Applications," Biosensors, vol. 12, p. 1183, 2022.

[7] A. M. Chiorcea-Paquim and A. M. Oliveira-Brett, "DNA Electrochemical Biosensors for In Situ Probing of Pharmaceutical Drug Oxidative DNA Damage," Sensors (Basel), vol. 21, Feb 5 2021.

[8] M. Banakar, M. Hamidi, Z. Khurshid, M. S. Zafar, J. Sapkota, R. Azizian, et al., "Electrochemical Biosensors for Pathogen Detection: An Updated Review," Biosensors (Basel), vol. 12, Oct 26 2022.

[9] I. G. Munteanu and C. Apetrei, "A Review on Electrochemical Sensors and Biosensors Used in Assessing Antioxidant Activity," Antioxidants (Basel), vol. 11, Mar 18 2022.

[10] A. Borchers and T. Pieler, "Programming pluripotent precursor cells derived from Xenopus embryos to generate specific tissues and organs," Genes (Basel), vol. 1, pp. 413-26, Nov 18 2010.

[11] S. S. Mahshid, S. E. Flynn, and S. Mahshid, "The potential application of electrochemical biosensors in the COVID-19 pandemic: A perspective on the rapid diagnostics of SARS-CoV-2," Biosens Bioelectron, vol. 176, p. 112905, Mar 15 2021.

[12] B. Perez-Fernandez and A. de la Escosura-Muniz, "Electrochemical biosensors based on nanomaterials for aflatoxins detection: A review (2015-2021)," Anal Chim Acta, vol. 1212, p. 339658, Jun 15 2022.
[13] Z. Lukács and T. Kristóf, "A generalized model of the equivalent circuits in the electrochemical impedance spectroscopy," Electrochimica Acta, vol. 363, p. 137199, 2020.
[14] L. Lopez, N. Hernandez, J. Reyes Morales, J. Cruz, K. Flores, J. Gonzalez-Amoretti, et al., "Measurement of Neuropeptide Y Using Aptamer-Modified Microelectrodes by Electrochemical Impedance Spectroscopy," Anal Chem, vol. 93, pp. 973-980, Jan 19 2021.
[15] Z.-B. Chen, H.-H. Jin, Z.-G. Yang, and D.-P. He, "Recent advances on bioreceptors and metal nanomaterials-based electrochemical impedance spectroscopy biosensors," Rare Metals, vol. 42, pp. 1098-1117, 2023.
[16] R. L. McCreery, "Advanced Carbon Electrode Materials for Molecular Electrochemistry," Chemical Reviews, vol. 108, pp. 2646-2687, 2008/07/01 2008.
[17] A. Benvidi, M. D. Tezerjani, S. Jahanbani, M. Mazloum Ardakani, and S. M. Moshtaghioun, "Comparison of impedimetric detection of DNA hybridization on the various biosensors based on modified glassy carbon electrodes with PANHS and nanomaterials of RGO and MWCNTs," Talanta, vol. 147, pp. 621-7, Jan 15 2016.
[18] A. García-Miranda Ferrari, S. J. Rowley-Neale, and C. E. Banks, "Screen-printed electrodes: Transitioning the laboratory in-to-the field," Talanta Open, vol. 3, p. 100032, 2021.
[19] G. Liang, Z. He, J. Zhen, H. Tian, L. Ai, L. Pan, et al., "Development of the screen-printed electrodes: A mini review on the application for pesticide detection," Environmental Technology & Innovation, vol. 28, p. 102922, 2022.
[20] G. Paimard, E. Ghasali, and M. Baeza, "Screen-Printed Electrodes: Fabrication, Modification, and Biosensing Applications," Chemosensors, vol. 11, p. 113, 2023.
[21] Sudesh, N. Kumar, S. Das, C. Bernhard, and G. D. Varma, "Effect of graphene oxide doping on superconducting properties of bulk MgB2," Superconductor Science and Technology, vol. 26, p. 095008, 2013.
[22] C. Valencia, C. H. Valencia, F. Zuluaga, M. E. Valencia, J. H. Mina, and C. D. Grande-Tovar, "Synthesis and Application of Scaffolds of Chitosan-Graphene Oxide by the Freeze-Drying Method for Tissue Regeneration," Molecules, vol. 23, Oct 16 2018.
[23] S. Jaworski, M. Wierzbicki, E. Sawosz, A. Jung, G. Gielerak, J. Biernat, et al., "Graphene Oxide-Based Nanocomposites Decorated with Silver Nanoparticles as an Antibacterial Agent," Nanoscale Res Lett, vol. 13, p. 116, Apr 23 2018.
[24] S. Muhammad Hafiz, R. Ritikos, T. J. Whitcher, N. Md. Razib, D. C. S. Bien, N. Chanlek, et al., "A practical carbon dioxide gas sensor using room-temperature hydrogen plasma reduced graphene oxide," Sensors and Actuators B: Chemical, vol. 193, pp. 692-700, 2014.
[25] S. Ameer and I. H. Gul, "Influence of Reduced Graphene Oxide on Effective Absorption Bandwidth Shift of Hybrid Absorbers," PLoS One, vol. 11, p. e0153544, 2016.
[26] S. A. Soomro, I. H. Gul, H. Naseer, S. Marwat, and M. Mujahid, "Improved Performance of CuFe2O4/rGO Nanohybrid as an Anode Material for Lithium-ion Batteries Prepared Via Facile One-step Method," Current Nanoscience, vol. 15, pp. 420-429, 2019.
[27] L. T. M. Thy, N. H. Thuong, T. H. Tu, N. H. T. My, H. H. P. Tuong, H. M. Nam, et al., "Fabrication and adsorption properties of magnetic graphene oxide nanocomposites for removal of arsenic (V) from water," Adsorption Science & Technology, vol. 38, pp. 240-253, 2020.
[28] A. Croitoru, O. Oprea, A. Nicoara, R. Trusca, M. Radu, I. Neacsu, et al., "Multifunctional Platforms Based on Graphene Oxide and Natural Products," Medicina, vol. 55, p. 230, 2019.
[29] E.A. Chiticaru, L. Pilan, C-M. Damian, E. Vasile, J.S. Burns, M. Ioniţă, "Influence of Graphene Oxide Concentration when Fabricating an Electrochemical Biosensor for DNA Detection", Biosensors. 2019; 9(4):113